# Growth and Characterization of Wurtzite GaAs Nanowires with Defect-Free Zinc Blende GaAsSb Inserts

**ARTICLE** *in* NANO LETTERS · JANUARY 2009

Impact Factor: 13.59 · DOI: 10.1021/nl802406d · Source: PubMed



**9 AUTHORS**, INCLUDING:

Dasa L Dheeraj
Crayonano AS
**38** PUBLICATIONS **630** CITATIONS
SEE PROFILE

Gilles Patriarche
French National Centre for Scientific Resea…
**543** PUBLICATIONS **6,307** CITATIONS
SEE PROFILE

Hailong Zhou
University of California, Los Angeles
**61** PUBLICATIONS **1,848** CITATIONS
SEE PROFILE

Helge Weman
Norwegian University of Science and Tech…
**132** PUBLICATIONS **1,426** CITATIONS
SEE PROFILE

NANO LETTERS



Letter

# Growth and Characterization of Wurtzite GaAs Nanowires with Defect-Free Zinc Blende GaAsSb Inserts

Dasa L. Dheeraj, Gilles Patriarche, Hailong Zhou, Thang B. Hoang, Anthonysamy F. Moses, Sondre Grønsberg, Antonius T. J. van Helvoort, Bjørn-Ove Fimland, and Helge Weman

*Nano Lett.*, **Article ASAP** • DOI: 10.1021/nl802406d



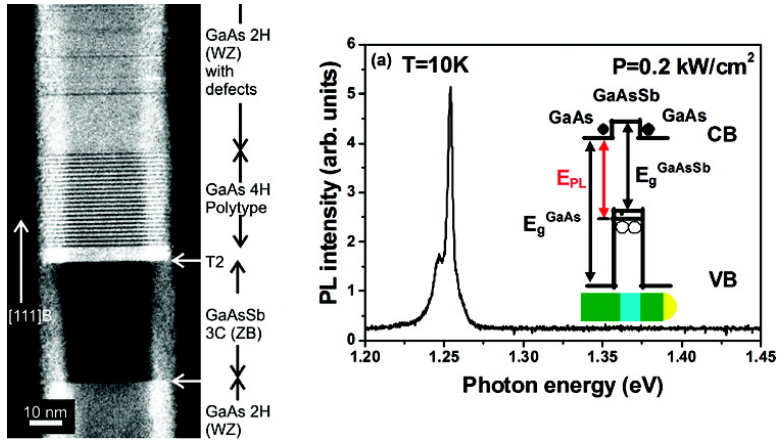


## More About This Article

Additional resources and features associated with this article are available within the HTML version:

- Supporting Information
- Access to high resolution figures
- Links to articles and content related to this article
- Copyright permission to reproduce figures and/or text from this article

View the Full Text HTML

NANO
LETTERS

XXXX
Vol. xx, No. x
-

# Growth and Characterization of Wurtzite GaAs Nanowires with Defect-Free Zinc Blende GaAsSb Inserts

**Dasa L. Dheeraj,[†] Gilles Patriarche,[‡] Hailong Zhou,[†] Thang B. Hoang,[†] Anthonysamy F. Moses,[†] Sondre Grønsberg,[§] Antonius T. J. van Helvoort,[§] Bjørn-Ove Fimland,[†] and Helge Weman*[,†]**

*Department of Electronics and Telecommunications, Norwegian University of Science and Technology, NO-7491 Trondheim, Norway, CNRS-LPN, Route de Nozay, F-91460 Marcoussis, France, Department of Physics, Norwegian University of Science and Technology, NO-7491 Trondheim, Norway*

*Received August 7, 2008; Revised Manuscript Received September 12, 2008*

**ABSTRACT**

**We have demonstrated the growth of a unique wurtzite (WZ) GaAs nanowire (NW) with a zinc blende (ZB) GaAsSb insert by Au-assisted molecular beam epitaxy. An abrupt interface from the WZ GaAs phase to the ZB GaAsSb phase was observed, whereas an intermediate segment of a 4H polytype GaAs phase was found directly above the ZB GaAsSb insert. A possible mechanism for the different phase transitions is discussed. Furthermore, low temperature microphotoluminescence ($\mu$-PL) measurements showed evidence of quantum confinement of holes in the GaAsSb insert.**

One dimensional (1D) NW heterostructures are very attractive research objects, promising for future nanoscaled electronic, opto-electronic, as well as thermoelectric device applications.[1,2] A diversity of NW heterostructures of both the III−V and IV groups, such as GaAs/GaP, InAs/InP, GaAs/GaSb, and Si/SiGe, have been fabricated.[1,3−5] A NW heterostructure is made by inserting one material (segment A) into the other (segment B). The band offset between the different segments provides possibilities to form heterojunctions and superlattices along the NW axis. Successful implementation of such NW heterostructures for devices requires being able to modulate the axial structure and composition of the NWs, and form abrupt interfaces between the segments. Among various growth techniques, molecular beam epitaxy (MBE) is one of the techniques that can be used to grow such axial heterostructures with atomic accuracy. Ternary III−V heterostructured NWs such as InP/InAsP,[6] GaP/GaAsP,[7] and core−shell AlGaAs,[8] were successfully grown by MBE using a metal catalyzed vapor−liquid−solid (VLS) mechanism.

The ZB phase is normally the most stable crystal structure observed in bulk III−V semiconductors. However, the crystal structure of [111]B-oriented III−V NWs grown by MBE is generally dominated by the WZ phase, often with stacking faults.[9,10] These defects may induce strong nonradiative recombination and decrease the luminescence efficiency and are thus a detrimental problem for optical device applications using NWs. To control the growth of NWs with a pure defect-free crystalline phase remains a challenging task. Recently, we reported on the growth of ZB GaAsSb NWs on [111]B-oriented GaAs with defect-free segments as long as 500 nm, which provides a possibility to make defect free GaAsSb inserts in GaAs/GaAsSb NW superlattice (NWSL) structures.[11] Periodic alternations in the crystal structure along a specific orientation forms a superlattice, which contains stacking of alternating segments $S_1$ and $S_2$ to a structure $S_1S_2S_1S_2S_1S_2...$ . The common NWSLs show either a chemical content variation (e.g., $S_1$ = InAs, $S_2$ = InP,[3] where both $S_1$ and $S_2$ exhibit the same crystal structure) or show the change of the crystalline structure (e.g., ZB versus WZ with same chemical composition). A so-called twinning superlattice which has the same structure and composition but differ in the relative orientation of the crystal direction along the NW, was reported recently.[12,13]

In this Letter, we report the growth of axial GaAs/GaAsSb heterostructured NWs with single GaAsSb inserts grown on GaAs (111)B substrates by Au-assisted MBE. The crystal structure along the NW changed from WZ to ZB when the GaAsSb insert was grown. The crystalline structure and the

* Corresponding author. E-mail: helge.weman@iet.ntnu.no.
[†] Department of Electronics and Telecommunications, Norwegian University of Science and Technology.
[‡] CNRS-LPN.
[§] Department of Physics, Norwegian University of Science and Technology.

10.1021/nl802406d CCC: $40.75 

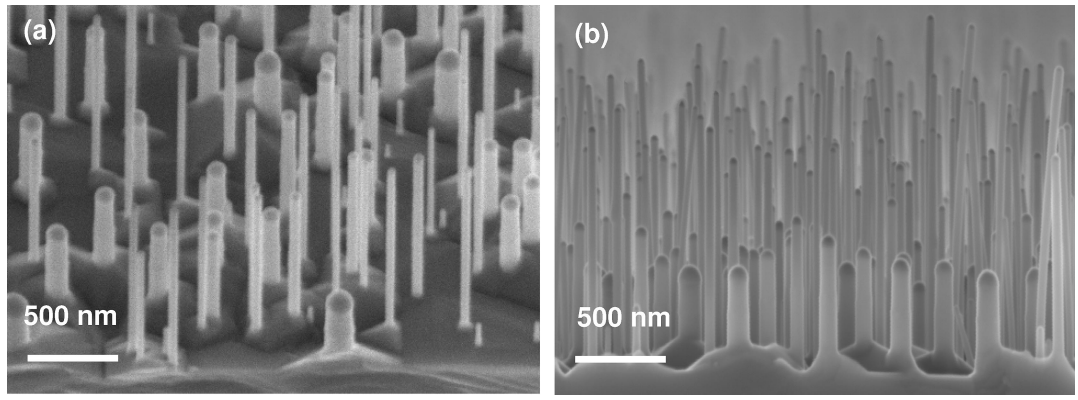


**Figure 1.** (a) 45° tilted view and (b) cross-sectional view SEM images of GaAs/GaAsSb heterostructured NWs grown on GaAs (111)B by Au-assisted MBE.

chemical composition were thus simultaneously altered along the NW. This could be a promising approach to realize a new type of NWSL structures. Moreover, the length of the insert, the period of the heterostructured NWs and the incorporation of Sb can be instantly controlled during the VLS growth. The dimensions of the NWs were investigated by scanning electron microscopy (SEM). Structural characterization of single NWs was done by high resolution transmission electron microscopy (HRTEM). Low temperature (10 K) $\mu$-PL performed on single NWs showed bright and narrow emission from the GaAsSb insert, indicating a high radiative efficiency even without using a passivating shell.

The GaAs/GaAsSb heterostructured NWs were grown in a Varian Gen II modular MBE system equipped with solid state Ga source and crackers of Sb and As, allowing fixing of the proportion of dimers and tetramers. In the present study, the major species of arsenic and antimony were $As_4$ and $Sb_2$, respectively. The substrate surface was first deoxidized at 620 °C, and then a ~200 nm thick GaAs buffer layer was grown. This buffer layer was capped with an amorphous As layer to avoid oxidation during its transfer in ambient air to an electron-beam evaporation system for gold depositions. After the As cap was desorbed under high vacuum ($\sim 10^{-7}$ Torr) in the electron-beam evaporation chamber, a ~1 nm thick Au film was deposited on the sample surface before the sample was loaded into the MBE system again.[11] Under an $As_4$ flux of $6 \times 10^{-6}$ Torr, the substrate temperature was increased to a temperature suitable for GaAs NW growth. At this stage, nanoparticles containing Au alloyed with the substrate constituents were formed. GaAs NW growth was initiated by opening the shutter of the Ga effusion cell. The temperature of the Ga effusion cell was preset to yield the required Ga flux. To form the GaAsSb NW insert, the Sb shutter was opened to supply an $Sb_2$ flux of $6 \times 10^{-7}$ Torr. The GaAs/GaAsSb heterostructured NWs were grown under a Ga flux of $3.5 \times 10^{-7}$ Torr and a substrate temperature of 540 °C. The GaAsSb insert was grown during 30 s after 20 min of GaAs NW growth and was followed by 5 min of GaAs NW growth. We did not perform any growth interruption at the heterointerfaces.

Morphological characterization of NWs was performed in a Zeiss Supra field emission scanning electron microscope (FE-SEM) operating at 5 kV. The NWs were analyzed in a Philips CM20 and a CM30 TEM (both $LaB_6$) both operating at 200 kV. The CM20 was equipped with an Oxford instruments INCA energy dispersive X-ray (EDX) spectrometer. For TEM characterization, the NWs were scraped off from the substrate and transferred to a Cu grid with a lacey carbon support film.

For $\mu$-PL, samples were placed in a continuous liquid He flow cryostat (10 K) and excited with a continuous wave Ar-ion laser (514 nm). The laser was focused onto the samples with an excitation density varied between 0.2 and 1.1 kW $cm^{-2}$ using a long working distance objective lens with a numerical aperture of 0.5 (spot size of ~1 $\mu$m) and a magnification of 50×. The $\mu$-PL from single NWs was dispersed by a 0.46 m focal length spectrometer and detected by a nitrogen-cooled Si CCD camera. For single NW measurements, NWs were removed from their grown substrate and dispersed on a Si substrate with the average density of ~0.1 NW per $\mu m^2$.

Figure 1 depicts the 45° tilted view (a) and cross-sectional view (b) SEM images of GaAs NWs with a single GaAsSb insert. The diameter of the NWs is in the range from 40 to 120 nm and the length of the NWs varies from 0.5 to 1 $\mu$m. As can be seen from the SEM images (Figures 1a,b), there is a large distribution in diameter and length of the NWs.

Figure 2a shows the [11$\bar{2}$0] oriented (WZ) dark field image of a typical GaAs NW with a single ZB GaAsSb insert. The dark field is taken around 2H (1$\bar{1}$00) WZ reflection, and it includes reflections from the microtwin and 4H polytype (see below) but no reflections from the ZB GaAsSb insert. The lengths of the GaAsSb inserts were observed to decrease with the increase in diameter of the NWs, as shown in Figure 3. The average length of the GaAsSb insert is about 30 nm. This observation is similar to the relation between the total length and diameter of the NWs. The shape of the length−diameter curve is similar to the observation for GaAsSb[11] and GaAs NWs.[14] For the GaAsSb inserts, a $1/R$ behavior, indicated by the solid line in Figure 3, of the length is observed. This indicates that the NW growth is induced by the diffusion of the adatoms on the sidewalls of the NW, in accordance with the VLS growth model proposed by Dubrovskii and Sibirev.[15]

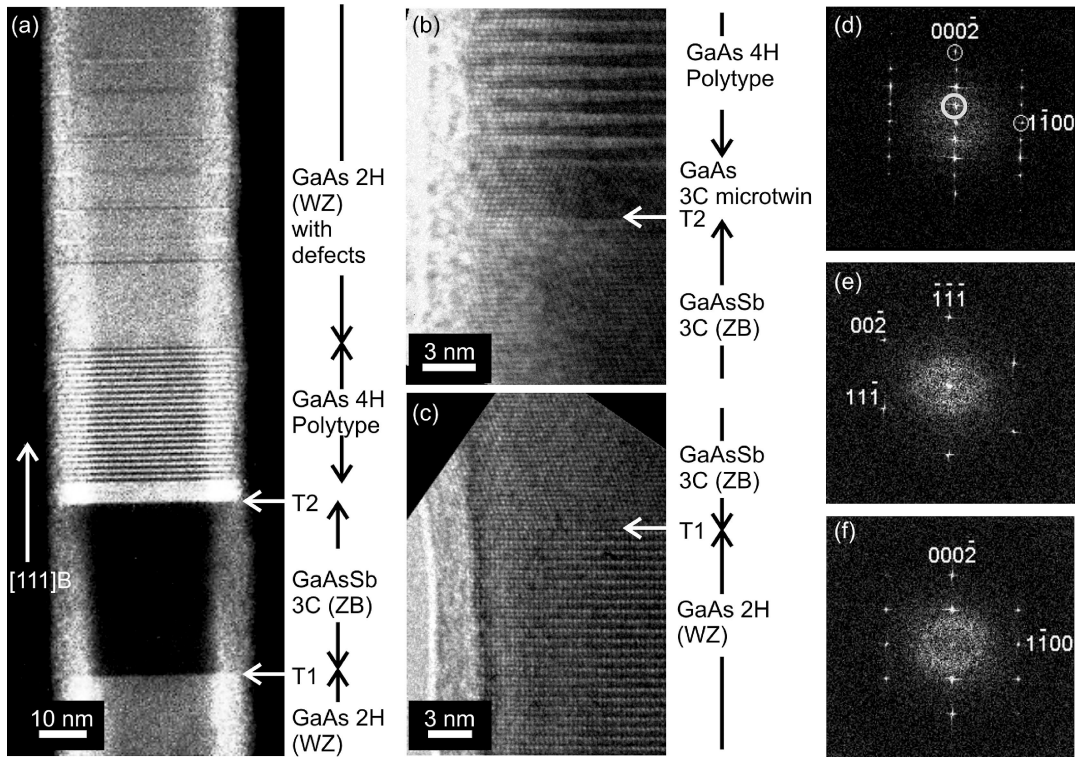


**Figure 2.** TEM images taken from the typical [111]B-oriented heterostructured GaAs/GaAsSb NWs. (a) Dark field TEM around 2H ($1\bar{1}00$) reflection (no reflection from the GaAsSb insert), which reveals the WZ phase of GaAs, ZB phase of the GaAsSb insert, GaAs 3C microtwin phase, and GaAs 4H polytype phase. The T1 and T2 GaAs/GaAsSb interfaces are pointed out with white arrows. (b) HRTEM image around interface T2, (c) HRTEM image around interface T1. (d,e,f) Fast Fourier transforms (FFT) of HRTEM images of the GaAs 4H polytype above the insert, the GaAsSb ZB insert, and the GaAs WZ phases below the insert, respectively. Thick circle in (d) indicates the $^1/_4(0002)$ reflection characteristic for a 4H polytype phase, whereas the two thin gray circles show the ($1\bar{1}00$) and ($000\bar{2}$) reflections characteristic for a WZ phase.

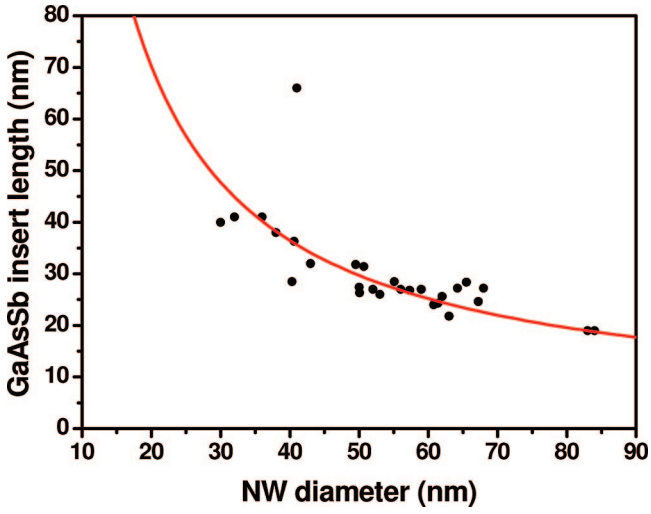


**Figure 3.** The length of the single GaAsSb insert as a function of the NW diameter. The solid line is a simulation according to the VLS growth model proposed by Dubrovskii and Sibirev.[15]

The GaAs NW segment before the GaAsSb insert exhibits a pure WZ phase with almost no stacking faults. As can be seen in Figure 2a and the HRTEM of Figure 2c, the transition (marked as T1) from the GaAs WZ phase to the GaAsSb ZB phase insert is very abrupt. In about $^1/_3$ of the studied NWs, a short (<5 nm) twinned ZB transition region is observed at the start of the GaAsSb ZB insert. The second transition from the GaAsSb ZB insert to the upper GaAs NW segment (marked as T2), is shown by HRTEM in Figure 2b. In most of the NWs, the defect-free GaAsSb ZB insert is directly followed by a few nanometers of a twinned GaAs cubic phase (ZB/3C). Above this microtwin, a GaAs 4H polytype phase is formed before the GaAs NW segment again returned to a WZ phase. The length of the GaAs 4H polytype phase varies between 20 and 40 nm depending on the NW diameter. The WZ phase of the upper GaAs NW segment contains randomly spaced stacking faults, small regions of 4H, and twinned ZB as can be seen in Figure 2a. Fast Fourier transforms on HRTEM images of the 4H, ZB, and WZ phases are shown in parts d, e, and f of Figure 2, respectively. The appearance of a $^1/_4(0002)$ reflection in Figure 2d (indicated by a thick circle) confirms a GaAs 4H polytype phase with the stacking sequence of ABCBA... . The EDX analysis was performed on the entire NW, including the segment after the GaAsSb insert, as well as on the gold droplet. Sb was only found in the GaAsSb insert. Furthermore, the Sb mole fraction of the GaAsSb inserts for different NWs was found to be in the range from 6 to 25%. Composition fluctuation from NW to NW could be due to the size distribution of their diameter and/or to their local NW environment during growth.

The 4H polytype structure is well-known in bulk form in wide band gap materials such as SiC and AlN. The 4H polytype of SiC is studied in detail due to its superior electron mobility.[16] The understanding of the NW growth conditions

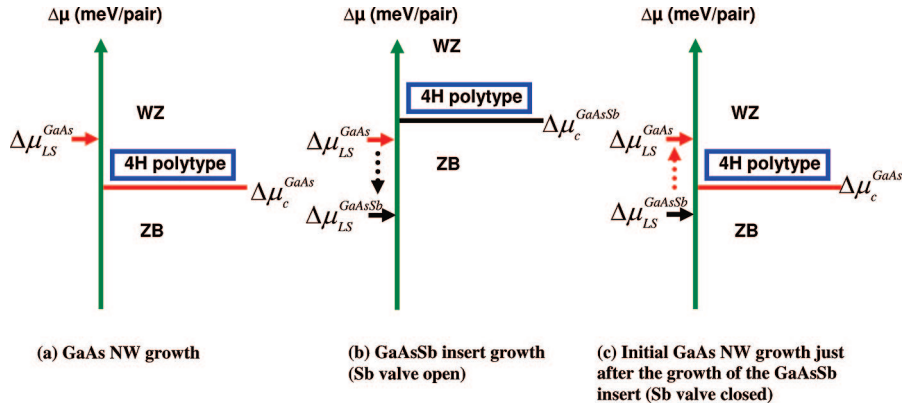


**Figure 4.** Schematic illustrations of a proposed mechanism for the occurrence of the different observed phase transitions. The possible configurations of the chemical potential difference (supersaturation) $\Delta\mu_{LS}$ (red arrow) and material-dependent critical supersaturation $\Delta\mu_c$ (black arrow) are indicated during (a) GaAs NW growth, (b) GaAsSb insert growth (Sb valve open), and (c) initial GaAs NW growth just after the growth of the GaAsSb insert (Sb valve closed).

favoring the formation of the 4H polytype in III−V materials that normally grow with a cubic ZB phase is thus an intriguing topic. The presence of a 4H polytype phase in GaAs and AlGaAs NWs was shown by Soshnikov et al.[17] We believe that the 4H polytype is the intermediate phase between the ZB and WZ phases. As suggested by Dubrovskii et al.,[19] the gradual change in the supersaturation conditions could lead to the formation of intermediate structures such as cubic twins and a 4H polytype phase and delay the formation of the WZ phase. It is reasonable to believe that the supersaturation is gradually increasing after the shut off of the Sb flux and that this induces the 4H polytype crystal structure. However, no traces of Sb were found above the insert, nor in the gold particle, as mentioned above.

In our recent report on the growth of ZB GaAsSb NWs, we found that on the introduction of Sb into the growth chamber, the ZB phase can be favorably formed due to two reasons: the first, decrease in chemical potential difference (supersaturation) $\Delta\mu_{LS}$ of the liquid (L) phase with respect to the solid (S) phase, and the second, increase in a material-dependent critical supersaturation value $\Delta\mu_c$.[11] The formation of ZB structured GaAsSb could thus be due to either an decrease of $\Delta\mu_{LS}$ or an increase of $\Delta\mu_c$ (or both). According to the HRTEM results, the most likely explanation for the phase transitions at the interfaces (T1 and T2) is that they are induced by the changing of both $\Delta\mu_c$ and $\Delta\mu_{LS}$ due to the introduction of Sb flux while growing. It should be noted that the chemical potential difference (supersaturation) $\Delta\mu_{LS}$ is gradually varying with time when the Sb flux is opened or closed, whereas the material-dependent critical supersaturation value $\Delta\mu_c$ is instantaneously changed between its corresponding values $\Delta\mu_{LS}^{GaAsSb}$ and $\Delta\mu_{LS}^{GaAs}$ for GaAsSb and GaAs, respectively. We believe that this is the main reason for forming two different interfaces at T1 and T2, and the detailed discussion is described in the following. According to the NW growth models by Glas et al.[18] and Dubrovskii et al.,[19] the supersaturation value for the Au liquid droplet ($\Delta\mu$) required to nucleate the 4H polytype phase is higher than that for the ZB phase, and the WZ phase is higher than that for the 4H polytype phase, as shown in Figure 4. As the GaAs NW grows, the chemical potential difference $\Delta\mu_{LS}$ is $\Delta\mu_{LS}^{GaAs}$ in the WZ phase region (indicated with a red arrow in Figure 4a). At the start of the GaAsSb insert growth, the critical supersaturation value $\Delta\mu_c$ instantaneously increases to the value required for the formation of the GaAsSb ZB phase ($\Delta\mu_c^{GaAsSb}$), whereas the chemical potential difference needs some time to gradually decrease to the equilibrium condition ($\Delta\mu_{LS}^{GaAsSb}$, indicated by a black arrow in Figure 4b) for the formation of the GaAsSb ZB phase. However, the NWs should have ZB phase after introducing Sb into the MBE chamber due to that $\Delta\mu < \Delta\mu_c^{GaAsSb}$, and hence a sharp interface occurs at T1. Reversely, after turning off the Sb flux, even though $\Delta\mu_c$ instantaneously goes back to $\Delta\mu_c^{GaAs}$, as shown in Figure 4c, $\Delta\mu_{LS}$ gradually increases to the supersaturation condition $\Delta\mu_{LS}^{GaAs}$. This gradual change in the supersaturation condition could lead to the formation of intermediate structures such as cubic twins and 4H polytype and thus delay the formation of the WZ phase.[19] This is, however, just one possible explanation for why there are two different GaAs/GaAsSb interface transitions (at T1 and T2) based on our HRTEM observations and does not yet give a complete description of the actual variations of $\Delta\mu_{LS}$ and $\Delta\mu_c$.

Figure 5a shows a $\mu$-PL emission spectrum from a single GaAs/GaAsSb heterostructured NW. The spectrum shows a sharp (~4 meV full width at half-maximum) emission at 1.254 eV at low excitation power (~0.2 kW/cm$^2$), coming from the GaAsSb insert. The emission at lower energy, which appears as a shoulder in Figure 5a, is believed to be due to NW surface effects or defects. On the other hand, no emission at higher energies around the GaAs band gap region (around 1.52 eV) was observed in this NW. As has previously been reported for GaAs/GaAsSb quantum wells,[20] the band alignment is a staggered type II, with the conduction and valence band offsets as illustrated in the inset of Figure 5a. We therefore believe that the narrow PL emission observed in Figure 5a is due to exciton recombination between confined holes in the GaAsSb insert and electrons in the GaAs NW segments at the GaAs/GaAsSb interfaces. However, to confirm that the GaAsSb insert emission is due to a type II recombination, time-resolved measurement of the radiative lifetime is needed. Our present NW hetero-

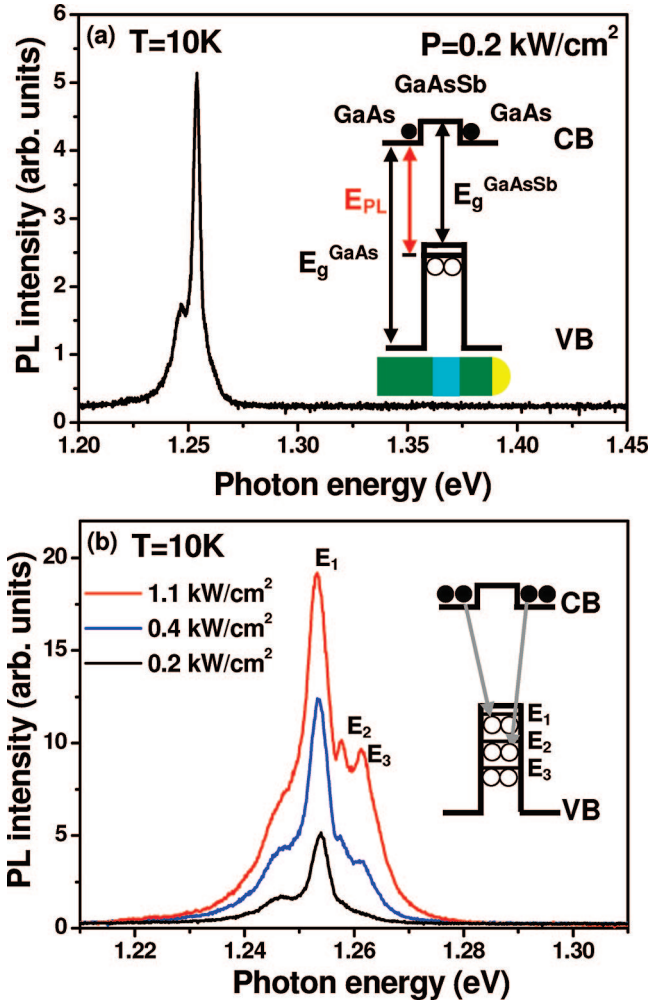


**Figure 5.** (a) Low temperature (10 K) $\mu$-PL emission spectrum from a single GaAs/GaAsSb heterostructured NW at (a) a power density of 0.2 kW/cm$^2$ and (b) at power densities of 0.2, 0.4, and 1.1 kW/cm$^2$. Insets show schematic pictures to present the band gap alignment and PL transition in a staggered type II GaAs/GaAsSb heterojunction. Filled and open dots indicate electrons and holes, respectively.

structure is, however, not ideal for such measurements because of an expected large influence of nonradiative surface recombination. Figure 5b shows the excitation power dependent $\mu$-PL emission from the GaAsSb insert on the same NW as presented in Figure 5a, where two higher energy peaks at 1.258 ($E_2$) and 1.262 eV ($E_3$) are observed. We attribute these higher energy peaks to the recombination to higher excited hole levels in the GaAsSb insert (as illustrated in the inset of Figure 5b). However, further investigation of these excited states is needed, together with modeling of the confinement potential, to clarify their origin.

In conclusion, GaAs/GaAsSb heterostructured NW were grown by MBE using the Au-assisted VLS method. HRTEM studies show the GaAsSb inserts to be defect free and of ZB phase. Also, the crystal phase transition was observed to be abrupt at the WZ GaAs to ZB GaAsSb lower interface, whereas an intermediate 4H polytype phase was observed in the GaAs segment above the GaAsSb upper interface. The average length of the GaAsSb ZB insert is about 30 nm, and the length of the GaAs 4H polytype phase is around 20−40 nm. The main reason for the difference in the two phase transitions is believed to be the combination of the gradual change of the chemical potential difference (supersaturation) $\Delta\mu_{LS}$ and the abrupt change of the material-dependent critical supersaturation value $\Delta\mu_c$ when the Sb flux is turned on or off. Low temperature $\mu$-PL measurements on a single NW show a strong, sharp type II emission from the GaAsSb insert at 1.254 eV. The ability to grow NW superlattices with alternating crystal structures and band gaps creates new possibilities for further development of single NW devices.

**Acknowledgment.** Part of this work was supported by the "NANOMAT" program (grant no. 182091) and the Norwegian−French "AURORA" program (grant no. 187692) of the Research Council of Norway.

## References

(1) Gudiksen, M. S.; Lauhon, L. J.; Wang, J.; Smith, D. C.; Lieber, C. M. *Nature* **2002**, *415*, 617–620.
(2) Robinson, R. D.; Sadtler, B.; Demchenko, D. O.; Erdonmez, C. K.; Wang, L.-W.; Paul, A. A. *Science* **2007**, *317*, 355–358.
(3) Björk, M. T.; Ohlsson, B. J.; Sass, T.; Persson, A. I.; Thelander, C.; Magnusson, M. H.; Deppert, K.; Wallenberg, L. R.; Samuelson, L. *Nano Lett.* **2002**, *2*, 87–89.
(4) Wu, Y.; Fan, R.; Yang, P. *Nano Lett.* **2002**, *2*, 83–86.
(5) Guo, Y. N.; Zou, J.; Paladugu, M.; Wang, H.; Gao, Q.; Tan, H. H.; Jagadish, C. *Appl. Phys. Lett.* **2006**, *89*, 231917–23919.
(6) Tchernycheva, M.; Cirlin, G. E.; Patriarche, G.; Travers, L.; Zwiller, V.; Perinetti, U.; Harmand, J. C. *Nano Lett.* **2007**, *7*, 1500–1504.
(7) Mohseni, P. K.; Maunders, C.; Botton, G. A.; LaPierre, R. R. *Nanotechnology* **2007**, *18*, 445304–445309.
(8) Chen, C.; Shehata, S.; Fradin, C.; LaPierre, R.; Couteau, C.; Weihs, G. *Nano Lett.* **2007**, *7*, 2584–2589.
(9) Koguchi, M.; Kakibayashi, H.; Yasawa, M.; Hiruma, K.; Katsuyama, T. *Jpn. J. Appl. Phys.* **1992**, *31*, 2061–2065.
(10) Persson, A. I.; Larsson, M. W.; Stenström, S.; Ohlsson, B. J.; Samuelson, L.; Wallenberg, L. R. *Nat. Mater.* **2004**, *3*, 677–681.
(11) Dheeraj, D. L.; Patriarche, G.; Largeau, L.; Zhou, H. L.; van Helvoort, A. T. J.; Glas, F.; Harmand, J. C.; Fimland, B. O.; Weman, H. *Nanotechnology* **2008**, *19*, 275605–275608.
(12) Bao, J. M.; Bell, D. C.; Capasso, F.; Wagner, J. B.; Mårtensson, T.; Trägårdh, J.; Samuelson, L. *Nano Lett.* **2008**, *8*, 836–841.
(13) Xiong, Q. H.; Wang, J.; Eklund, P. C. *Nano Lett.* **2006**, *6*, 2736–2742.
(14) Plante, M. C.; LaPierre, R. R. *J. Cryst. Growth* **2006**, *286*, 394–399.
(15) Dubrovskii, V. G.; Sibirev, N. V. *J. Cryst. Growth* **2007**, *304*, 504–513.
(16) Meyer, B. K.; Hofmann, D. M.; Volm, D.; Chen, W. M.; Son, N. T.; Janzén, E. *Phys. Rev. B* **2001**, *61*, 4844–4849.
(17) Soshnikov, I. P.; Cirlin, G. E.; Tonkikh, A. A.; Samsonenko, Y. B.; Dubrovskii, V. G.; Ustinov, V. M.; Gorbenko, O. M.; Litvinov, D.; Gerthsen, D. *Phys. Solid State* **2005**, *47*, 2121–2126.
(18) Glas, F.; Harmand, J. C.; Patriarche, G. *Phys. Rev. Lett.* **2007**, *99*, 146101.
(19) Dubrovskii, V. G.; Sibirev, N. V. *Phys. Rev. B* **2008**, *77*, 035414–035418.
(20) Teissier, R.; Sicault, D.; Harmand, J. C.; Ungaro, G.; Le Roux, G.; Largeau, L. *J. Appl. Phys.* **2001**, *89*, 5473–5477.

NL802406D